References

[1]Schetz, J. A., Billig, F. S., and Favin, S., "Analysis of External Burning on Inclined Surfaces in Supersonic Flow," *Journal of Propulsion and Power*, Vol. 10, No. 5, 1994, pp. 602–608.

[2]Kahaner, D., Moler, C., and Nash, S., *Numerical Methods and Software*, Prentice–Hall, Englewood Cliffs, NJ, 1988, Chap. 8.

[3]Colasurdo, G., and Pastrone, D., "Indirect Optimization Method for Impulsive Transfers," AIAA/AAS Astrodynamic Conference, AIAA, Washington, DC, 1994, pp. 441–448; also AIAA Paper 94-3762, 1994.

Three-Dimensional Disturbance Vortex Method for Simulating Rotor/Stator Interaction in Turbomachinery

Xian Hong Wu*
Ben-Gurion University of the Negev, 84105 Beer-Sheva, Israel
and
Mao Zhang Chen†
Beijing University of Aeronautics and Astronautics, 100083 Beijing, People's Republic of China

I. Introduction

IT is necessary to account for three-dimensional unsteady flow effects in the design procedure to improve turbomachine performance and efficiency. The present trend toward closer blade-row spacing has emphasized the need for reliable techniques to resolve the unsteady flowfield. There are three dominant causes of unsteadiness relating to rotor and stator interaction. The first is the interaction between wakes and downstream blades. The second is the potential interaction between upstream and downstream blades. The third is the interaction between upstream vortex and downstream blades. For modern transonic turbomachines, as pointed out by Jung et al.,[1] if the velocity is sufficiently high at the interface between rotor and stator, the effects of upstream unsteadiness on the downstream are much stronger than that of the downstream on the upstream, and the disturbance is dominantly transported downstream. The disturbance vortex method for simulating two-dimensional rotor/stator interaction in turbomachinery has been presented by Wu and Chen,[2] where good agreement between the computational and experimental results is obtained. Therefore, it is natural to extend this method to three-dimensional domain. In view of its inherent advantages, such as treatment of the complex boundaries and application of the Baldwin–Lomax[3] turbulence model to wakes, the idea is developed to simulate three-dimensional unsteady flow in turbomachinery.

II. Numerical Method

Governing Equations

The vorticity dynamic equation for three-dimensional viscous flow is

$$\frac{\partial \omega}{\partial t} + (V \cdot \nabla)\omega = (\omega \cdot \nabla)V - \omega(\nabla \cdot V) + \nu\nabla^2\omega \qquad (1)$$

Substituting ω and V in Eq. (1) by $\omega = \bar{\Omega} + \omega'$ and $V = \bar{U} + u'$, respectively, one obtains

$$\frac{\partial \bar{\Omega}}{\partial t} + \frac{\partial \omega'}{\partial t} + (\bar{U} \cdot \nabla)\bar{\Omega} + (\bar{U} \cdot \nabla)\omega' + (u' \cdot \nabla)\bar{\Omega} + (u' \cdot \nabla)\omega'$$
$$= (\bar{\Omega} \cdot \nabla)\bar{U} + (\bar{\Omega} \cdot \nabla)u' + (\omega' \cdot \nabla)\bar{U} + (\omega' \cdot \nabla)u' - \bar{\Omega}(\nabla \cdot \bar{U})$$
$$-\bar{\Omega}(\nabla \cdot u') - \omega'(\nabla \cdot \bar{U}) - \omega'(\nabla \cdot u') + \nu\nabla^2\bar{\Omega} + \nu\nabla^2\omega' \qquad (2)$$

where $\bar{\Omega} = \nabla \times \bar{U}$ is time-averaged vorticity and $\omega' = \nabla \times u'$ is disturbance vorticity. If the Mach number of time-averaged velocity is not very high, we can assume the volume expansion corresponding to disturbance velocities is zero,

$$\nabla \cdot u' = 0 \qquad (3)$$

Further discussion about this assumption may be found in Ref. 2.

Performing a time-averaging operation to Eq. (2) and applying

$$\int_0^T q' \, dt = 0, \qquad (q = \omega, V)$$

the equation for disturbance vorticity can be obtained as

$$\frac{d\omega'}{dt} = -(u' \cdot \nabla)\bar{\Omega} + \overline{(u' \cdot \nabla)\omega'} + (\bar{\Omega} \cdot \nabla)u' + (\omega' \cdot \nabla)\bar{U}$$
$$+ (\omega' \cdot \nabla)u' - \overline{(\omega' \cdot \nabla)u'} - \omega'(\nabla \cdot \bar{U}) + \nu\nabla^2\omega' \qquad (4)$$

where d/dt is the material derivative. In the case of laminar flow, the viscosity $\nu = \nu_l$, whereas for turbulent flow $\nu = (\nu_l + \nu_t)$, where ν_l and ν_t are the laminar and turbulent viscosity.

Initial and Boundary Conditions

The initial condition can be specified as follows:

$$q'(r, \theta, z, t_0) = \begin{cases} \bar{Q}_r(r, \theta, z) - \bar{Q}_{(\mathrm{axi})}(r, z) & x = x_1 \\ 0 & x \neq x_1 \end{cases} \qquad (5)$$

where $\bar{Q}_{(\mathrm{axi})}$ is the circumferential averaged value of $\bar{Q}_r$, the relative steady solutions of the upstream rotor; $x(r, \theta, z)$ is the coordinate; and x_1 are the inlet points of the stator domain.

On the solid wall, the impenetrable and no-slip conditions should be satisfied (discussed subsequently).

At upstream boundary, the upstream boundary condition for disturbance variables at time t can be obtained in the same way as Eq. (5) is obtained,

$$q'(r, \theta, z, t) = \bar{Q}_r(r, \theta - \lambda t, z) - \bar{Q}_{(\mathrm{axi})}(r, z) \qquad (6)$$

where $t = t_0 + k\Delta t$, $(1 \le k \le M)$, $\Delta t = T/M$, λ is the angular velocity of the rotor, and $T = P_r / V_r$, is the time period where P_r is rotor blade spacing, V_r is the circumferential velocity of the rotor, and M is the number of time steps in one period.

For geometric boundaries in a single passage, if the rotor and stator have the same blade spacing, a simple periodic condition exists. If the blade spacings are different, for example, the rotor spacing is larger than that of the stator (see Fig. 1), the "phase-shift periodic boundary condition"[4] exists:

$$q(r, \theta, z, t) = q(r, \theta + \theta_s, z, t + \Delta T) \qquad (7)$$

where $\Delta T = (P_r - P_s)/V_r$, $\theta_s = P_s / r$, and P_s is the stator blade spacing.

Turbulence Model

As in two-dimensional domain,[2] the Baldwin and Lomax[3] turbulence model faces the same difficulties when it is used to calculate unsteady wake. One difficulty is that the computed viscosity in the outer region is much higher than that in the boundary regions. This is because there is a high vorticity region in the wakes so that $F(y)$,

Received 10 April 1999; revision received 18 May 1999; accepted for publication 21 June 1999.

*Research Fellow, P.O. Box 653, Department of Mechanical Engineering.
†Professor, Department of Jet Propulsion.

defined as $y|\omega|$, reaches its maximum in the outer layer of the boundary. To solve this problem, we redefine y_{max} as the smallest distance at which $F(y)$ meets the condition

$$\frac{dF}{dy} = 0 \tag{8}$$

Another difficulty is in continuously tracing the moving wake centerlines so as to obtain the perpendicular distance of y to the wake centerlines in calculating the Klebanoff factor. In the three-dimensional domain, the center points and the widths of the wakes are defined in the same way as those in the two-dimensional domain,[2] so that the positions of the wakes at any time can be determined by the Lagrangian method. In the outer layer of the boundary, the total turbulence viscosity should include the combined effects of boundary and wake; in the inner layer of the boundary, the effect of wakes is comparatively weak, and so its viscosity is negligible.

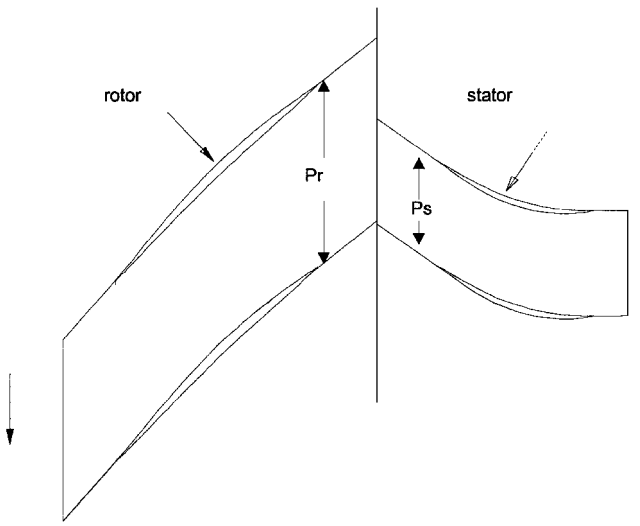

Fig. 1 Typical configuration of a single-stage compressor.

Computation Procedure

In the three-dimensional domain, the disturbance vorticity field can be represented by a set of discrete vortex particles,[5]

$$\omega'(x, t) = \sum_{j=1}^{N} \Gamma'_j f_\sigma[x - x_j(t)] \tag{9}$$

where N is the number of vortex particles and Γ'_j is the circulation. The smooth function $f_\sigma = (1/\sigma^3) f(x/\sigma)$, where σ is the radius of the vortex particle, and the shape function $f(x) = (3/4\pi)e^{-x^3}$. By the application of the viscous splitting algorithm,[5] the displacement and the circulation variation of the disturbance vortex caused by convective process are

$$x_2 = x_1 + (\bar{U} + u')\Delta t \tag{10}$$

$$\Gamma'(t + \Delta t) + \Gamma'(t) + F[-(u' \cdot \nabla)\bar{\Gamma} + (\bar{\Gamma} \cdot \nabla)u' + (\Gamma' \cdot \nabla)\bar{U} + (\Gamma' \cdot \nabla)u' - \overline{(\Gamma' \cdot \nabla)u'} - \Gamma'(\nabla \cdot \bar{U}) + \overline{(u' \cdot \nabla)\Gamma'}] \cdot \Delta t \tag{11}$$

where $F[\ ]$ is the integration scheme and $\bar{\Gamma}$ is the time-averaged circulation. The correlations $(\Gamma' \cdot \nabla)u'$ and $(u' \cdot \nabla)\Gamma'$ can be obtained through summing $(\Gamma' \cdot \nabla)u'$ and $(u' \cdot \nabla)\Gamma'$ of each time step and then performing a time-averaging operation in a period.

The contribution of the viscous term to the disturbance vorticity can be obtained by use of the random walk method.[5] The displacement caused by the viscous diffusion process is

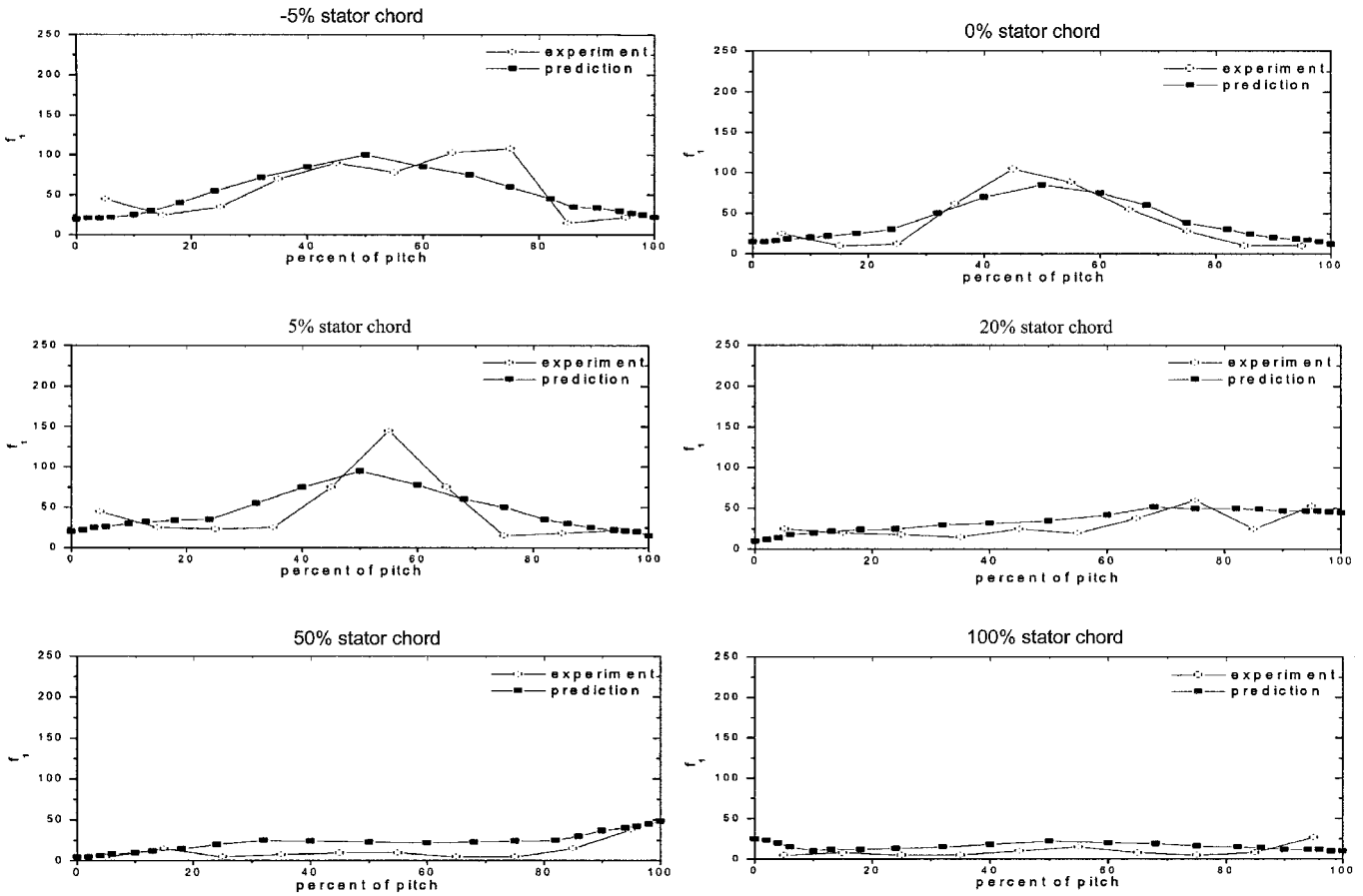

Fig. 2 Circumferential distribution of $\overline{u'^2}$ for NASA-67 compressor.

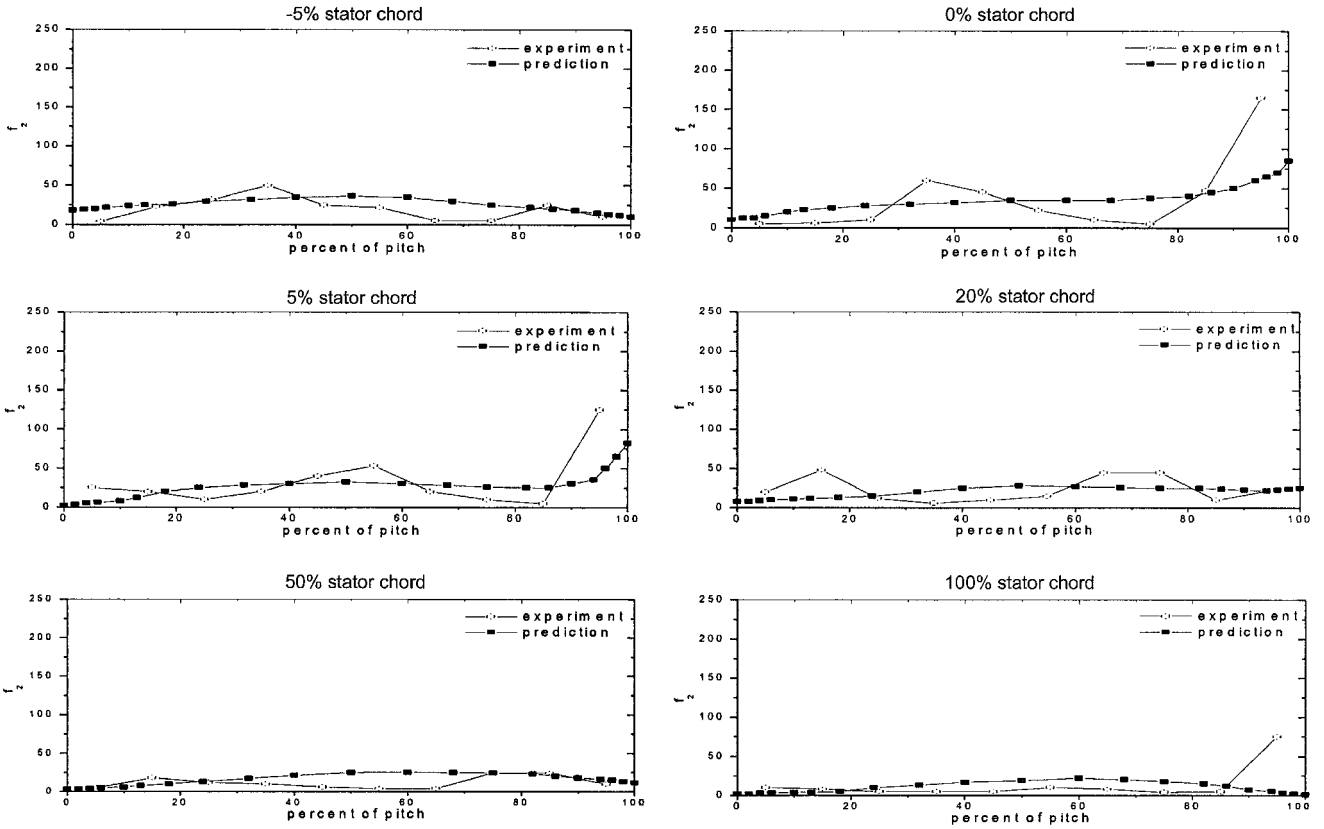

Fig. 3 Circumferential distribution of $\overline{v'^2}$ for NASA-67 compressor.

approximated by the random variables in each of the three coordinate directions, selected independently from a Gaussian distribution with zero mean and variance equal to $2\Delta t/Re$.

The disturbance velocity includes three parts: The first one, the disturbance velocity induced by the vortex particles, is evaluated as follows:

$$u'_v(x,t) = \sum_{j=1}^{N} K_\delta[x - x_j(t)] \wedge \Gamma'_j \tag{12}$$

where $\wedge$ stands for the convolution operator and $K_\sigma(x)$ is defined by Chorin.[5]

According to Batchelor,[6] if there exists the assumption of Eq. (3), the second disturbance velocity, associated with disturbance expansion, should be zero.

To meet the impenetrable condition on solid walls, a potential disturbance velocity (the third part) is added:

$$(u'_e + u'_v) \cdot n = -u'_p \cdot n \tag{13}$$

for the points $x \in B$, where B represents the solid surface. The potential disturbance velocity is defined as $\nabla\phi(x) = u'_p$, in which the potential function is the solution of the three-dimensional Laplace equation,

$$\nabla^2\phi = \frac{\partial^2\phi}{\partial r^2} + \frac{\partial^2\phi}{r^2\partial\theta^2} + \frac{\partial^2\phi}{\partial z^2} + \frac{\partial\phi}{r\partial r} = 0 \tag{14}$$

under the unsteady boundary condition on the geometric boundaries of Eq. (7). The no-slip condition on solid walls may be calculated as by Chorin[5] by creating new vortex sheets on the boundary. At any time step, the motion of vortex sheets at the boundary is determined.[5] Once they enter into the main flow region, they are converted into vortex particles keeping their vorticity strength unchanged. If vortex particles go into the boundary layer, their effects are negligible.

III. Validation of the Method

To check the present method, we calculated the unsteady flows due to rotor/stator interaction in the first stage of the NASA-67 compressor, which consists of 22 rotor blades and 34 stator blades. The results, unsteady velocity correlations u'^2 and v'^2 along the circumferential direction at the middle span, are compared with experimental data of Hathaway[7] at six axial positions: −5, 0, 5, 20, 50, and 100% of stator chord (see Figs. 2 and 3). Here −5% of chord represents the position 5% of stator chord in front of the leading edge of the stator. The same y axial scales for Figs. 2 and 3 were adopted so as to check the decaying characteristic along the streamwise direction. These contours show that the prediction and experimental data are in general agreement. From the prediction it may be concluded that the present method is reliable.

IV. Conclusion

The three-dimensional disturbance vortex method to simulate the unsteadiness caused by rotor/stator interaction in turbomachinery is presented in this paper. The Baldwin–Lomax turbulence model is applied to the wake to distinguish its viscous effect from that in the boundary layer. Numerical results show that the predicted results are in good agreement with the experimental data. We conclude that the disturbance vortex method presented can be used as a new tool for analyzing unsteady flow in turbomachinery.

References

[1]Jung, A. R., Mayer, J. F., and Stetter, H., "Simulation of 3D-Unsteady Stator/Rotor Interaction in Turbomachinery Stages of Arbitrary Pitch Ratio," American Society of Mechanical Engineers, Paper 96-GT-69, 1996.

[2]Wu, X., and Chen, M., "Vortex Simulation of Rotor/Stator Interaction in Turbomachinery," American Society of Mechanical Engineers, Paper 98-GT-15, 1998.

[3]Baldwin, B. S., and Lomax, H., "Thin Layer Approximation and Algebraic Model for Separated Turbulent Flows," AIAA Paper 78-257, 1978.

[4]Giles, M. B., "Stator/Rotor Interation in a Transonic Turbine," *Journal of Propulsion*, Vol. 6, No. 5, 1990, pp. 621–627.

[5]Chorin, A. J., "Numerical Study of Slightly Viscous Flow," *Journal of*

Fluid Mechanics, Vol. 57, 1973, pp. 785–796.
[6]Batchelor, G. K., *An Introduction to Fluid Dynamics*, Cambridge Univ. Press, New York, 1967.
[7]Hathaway, M. D., "Unsteady Flows in a Single-Stage Transonic Axial-Flow Fan Stator Row," NASA TM-88929, 1986.

Measurements of Turbulent Flow Structure in Supersonic Curved Wall Boundary Layers

R. D. W. Bowersox*
University of Alabama, Tuscaloosa, Alabama 35487
R. C. Wier†
U.S. Air Force Research Laboratory, Eglin Air Force Base, Florida 32542
D. D. Glawe‡
U.S. Air Force Research Laboratory, Wright–Patterson Air Force Base, Ohio 45433
and
S. Gogineni§
Innovative Scientific Solutions, Inc., Dayton, Ohio 45440

Introduction

THE underlying physics of high-speed flow over many of the shapes encountered on the interior surfaces of an engine are not well understood.[1,2] Thus, further experimental and related computational investigations are required to ascertain accurate predictions of the flow dynamics. The present paper discusses the results from an experimental study that examined energy spectral data and instantaneous (10 ns) Mie-scatting flow visualizations to quantify the effects of wall curvature on the large-scale turbulent boundary-layer flow structures for the curved wall configurations of Ref. 3. The pressure-gradient strength for high-speed flow is difficult to characterize.[2] Luker et al.[3] present a detailed discussion on pressure-strength characterization for the present curved wall models.

Facilities and Instrumentation

The tests were performed on the models and in the supersonic wind tunnel described by Luker et al.[3] The freestream Mach number was 2.8. The plenum chamber total pressure and total temperature were maintained at 0.219 ± 0.012 MPa and 295 ± 2 K, respectively. Luker et al.[3] have also shown the flowfield to be two dimensional for the current wind-tunnel models; hence, the present measurements were obtained along the tunnel centerline. The spectral measurements were acquired at the axial locations where previous laser Doppler velocimetry (LDV) data[3] were acquired, and the transverse locations were normal to the wall. The hot-wire instrumentation and procedures used here are described by Wier et al.[4]

A digital two-color particle image velocimetry (PIV) system was used for Mie-scattering flow visualization and preliminary PIV measurements.[5] The flow was seeded with triethylene-glycol smoke particles generated with a Dantec fog generator, where the polydisperse particles were confirmed to be less than 1.0 μm. Comparisons of preliminary PIV results with previous LDV results were performed to assess the flow tracking ability of the seed particles.[4] Even though the agreement with the LDV data was very good, the PIV velocity and turbulence intensity results were considered qualitative because of small sample sizes. Hence, only the instantaneous (10 ns) Mie-scattering images are described here.

Results and Discussion

The zero-pressure-gradient (ZPG), boundary-layer, large-scale turbulent flow structures visible in the boundary layers along the bottom walls shown in both Figs. 1a and 1b had inclination angles between 45 and 60 deg, which were similar to the results discussed by Spina,[6] and the structures spanned approximately one-half the boundary-layer thickness. Application of the adverse-pressure gradient (APG) (top wall, Fig. 1a) caused a decrease in the boundary-layer thickness and a reduction in the structure inclination angle (20–30 deg), where here the structures appeared to have spanned nearly the entire boundary layer. As the flow continued into the favorable-pressure-gradient region of this wall model, defined here as the combined-pressure-gradient (CPG) region, the boundary-layer thickness, the structure size and the structure angles began to grow in the x direction.

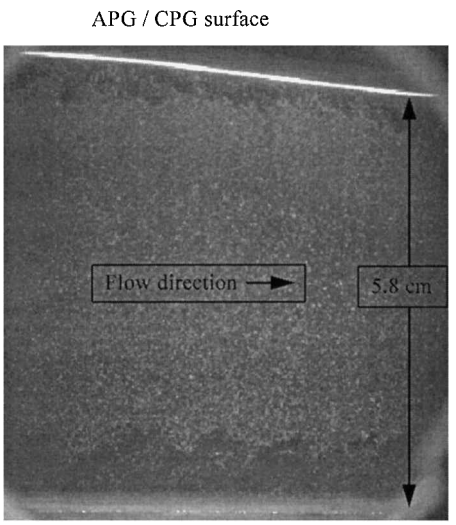

a) ZPG/APG/CPG

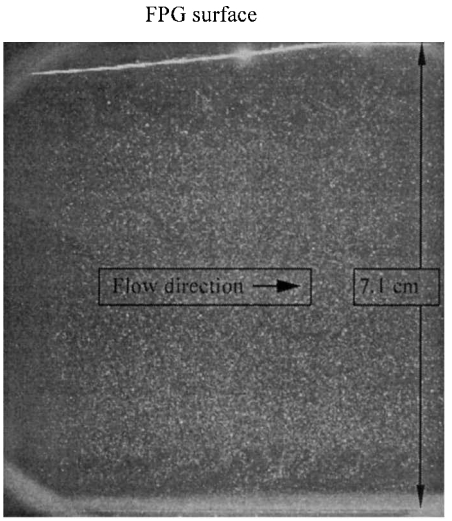

b) ZPG/FPG flow visualization

Fig. 1 Mie-scattering (PIV) flow visualizations.

Received 17 October 1998; revision received 5 July 1999; accepted for publication 14 September 1999. This material is declared a work of the U.S. Government and is not subject to copyright protection in the United States.
*Assistant Professor, Department of Aerospace Engineering and Mechanics.
†Aeronautical Engineer, Armament Directorate.
‡Experimental Research Engineer, Propulsion Sciences and Advanced Concepts Division.
§Senior Engineer, 2766 Indian Ripple Road.